Colloid Polym Sci 274:499–512 (1996)

ORIGINAL CONTRIBUTION

K.M. McGrath

Polymerisation of liquid crystalline phases in binary surfactant/water systems.

Part 3. Sodium 10-undecenoate

Received: 9 March 1995
Accepted: 26 October 1995

K.M. McGrath[1]
Department of Applied Mathematics
Research School of Physical Sciences
and Engineering
The Australian National University
Canberra ACT 0200, Australia

[1]*Present address*:
Dr. K.M. McGrath (✉)
Department of Physics
Princeton University
P.O. Box 708
Princeton, New Jersey 08544, USA

Abstract The polymerisation of a polymerisable fatty acid surfactant (sodium 10-undecenoate) has been studied in both its self-assembled and non self-assembled forms. Polymerisation in non self-assembled solution was achieved to near completion. The polymerisation produces a surface active polymer. The self-assembling behaviour of this pre-polymerised form differs markedly from that observed for the monomeric surfactant [1]. A lamellar phase only is formed in the polymeric phase diagram with no hexagonal or lamellar gel phases being observed. Polymerisation in the different self-assembled forms of sodium 10-undecenoate reached a limit of approximately 30% only, i.e., the surfactant aggregates act to inhibit the polymerisation. The nature of the hydrocarbon chain was found to play a critical role in determining the effect that polymerisation had on the underlying geometry of the surfactant molecules. When the chains are in a fluid-like state (as for the micellar and hexagonal phases) the original monomeric matrix remains largely unchanged. Whereas partial polymerisation of the lamellar gel phase results in a phase transformation.

In addition the hydrolysis of the fatty acid soap at low concentrations (close to the critical micelle concentration) has been investigated. Hydrolysis was shown to produce both the parent fatty acid and an acid soap dimer. The presence of these species greatly affects the solution behaviour in this region of the phase diagram shifting the critical micelle concentration to very high concentrations of sodium 10-undecenoate (ca. 0.4 M).

Key words Polymerisation – surfactant self-assembly – liquid crystals – sodium 10-undecenoate

Introduction

In the first two papers of this series [2, 3] the phase behaviour and polymerisation of three quaternary ammonium polymerisable surfactants has been discussed. This paper further extends this work by introducing a change in the nature of the head group to a fatty acid soap. Sodium 10-undecenoate (Na-10, $CH_2=CH-(CH_2)_8-CO_2^{-}Na^{+}$), like ω-undecenyltrimethylammonium bromide (ω-UTAB, $CH_2=CH-(CH_2)_9-N^{+}(CH_3)_3Br^{-}$, discussed in paper II of this series [3]), contains the allyl polymerisable moiety (a single carbon–carbon double bond) at the end of the hydrocarbon chain. The change in the nature of the head group from a quaternary ammonium to a carboxylate alters dramatically the self-assembly observed for the Na-10/water system [1] compared with that observed in the systems discussed previously [2, 3]. By comparing the physico-chemical behaviour of ω-UTAB [3] and Na-10, it should be possible

K 644

to determine the affect that the trimethylammonium bromide and sodium carboxylate head groups have on controlling the self-assembly of surfactant molecules and their polymerisation. Any observed difference in the two surfactants can only be attributed to changes in the interactions between the head groups and chain flexibility.

It has been shown [3] that the introduction of the allyl polymerisable group into the tail of the hydrocarbon chain does not significantly disturb the phase progression with changes in temperature and composition (ω-UTAB). Introduction of this group does, however, reduce both the solubility of the surfactant and the stability of the liquid crystalline phases. That is, the presence of a carbon–carbon double bond at the end of the hydrocarbon chain increases the rigidity of the chains. (Note that this is in contrast with the case where the double bond is incorporated into the beginning or middle of the chain where the flexibility of the chain is increased and the overall solubility of the surfactant is also increased [4]). This increased rigidity is expected to be magnified in the Na-10/water system since the effective chain length has been reduced still further as compared with ω-UTAB [3]. The influence of the allyl polymerisable moiety is therefore more dominant in this surfactant and the chain length is now more closely approximated by a C_8 or C_9 hydrocarbon chain, since the presence of a double bond is equivalent to reducing the chain length by approximately one CH_2 group [5]. Therefore, as the concentration of Na-10 is increased it is likely that an order/disorder transformation will be observed. This is indeed what happens and a transition between a normal hexagonal phase (H_α) and a lamellar gel phase occurs, with both the long- and short-range (that of the paraffinic chains) order being affected during the transition [1].

As well as the observed effect on the self-assembly of Na-10 caused by the combination of the position of the allyl polymerisable moiety, the presence of a fatty acid soap head group and a shortened chain length, the subsequent polymerisation should also be affected. Hydrocarbon chains in a fluid-like state have a high degree of mobility [6–15] unlike the case when the chains are frozen, where they are presumed to be almost crystalline in their nature [16–22]. Therefore, when the chains are in a fluid-like state polymerisation may retard their flexibility, whereas for frozen chains the number of degrees of freedom should be increased upon polymerisation. Hence, the nature of the paraffinic chains may have an affect upon the extent/ease of polymerisation of the liquid crystalline phases formed in the Na-10/water system and also on the degree of rearrangement which may occur during polymerisation.

Since Na-10 is the sodium salt of a fatty acid it is possible that in solution at low surfactant concentration several different forms of the surfactant will be present (i.e., the salt will undergo hydrolysis). These different forms consist of the parent fatty acid (undecenoic acid), the neutral soap and the charged carboxylate ion, due to dissociation of the sodium counterion. The presence of the parent fatty acid in the system will affect the initial aggregation of the surfactant and hence will be detectable by the methods used to determine the onset of aggregation of the surfactant, i.e., electrical conductivity and surface tension.

Experimental

Sodium 10-undecenoate (Na-10, $CH_2{=}CH{-}(CH_2)_8{-}CO_2^-$ Na^+) was prepared as described previously [23, 24]. Elemental Analysis: Calculated for $C_{11}H_{19}O_2Na$: C 64.08%; H 9.22%; O 15.53%; Na 11.17%. Found C 64.16% and H 9.38%. Decomposition temperature 220 °C. NMR Analysis: Proton $(C\underline{H}_2)_4^-(CH_2)_2{-}C{=}O$ 1.31 δ; $C\underline{H}_2{-}CH_2{-}CH{=}C$ 1.38 δ; $C\underline{H}_2{-}CH_2{-}C{=}O$ 1.56 δ; $C\underline{H}_2{-}CH{=}C$ 2.05 δ; $C\underline{H}_2{-}C{=}O$ 2.18 δ; $C\underline{H}_2{=}C$ doublet of doublets centred at 5.01 δ; $C\underline{H}{=}C$ 5.87 δ. Carbon 13 $\underline{C}H_2{-}C{=}O$ 25.78 δ; $(\underline{C}H_2)_5{-}CH_2{-}C{=}O$ 28.64 δ; $\underline{C}H_2{-}CH_2{-}C{=}O$ 33.12 δ; $\underline{C}H_2{-}CH{=}C$ 37.36 δ; $={\underline{C}}H_2$ 113.83 δ; $={\underline{C}}H$ 139.67 δ; $\underline{C}{=}O$ 183.55 δ. FTIR Analysis: Symmetric C=O carboxylate stretch 1462.5 cm^{-1}; asymmetric C=O carboxylate stretch 1560.0 cm^{-1}; C=C stretch 1642.8 cm^{-1}; H–C= stretch 3083.3 cm^{-1}.

All experimental techniques were as described in the first paper in this series [2].

Results

Critical micelle concentration

The electrical conductivity curve for the Na-10/water system at 25 °C is shown in Fig. 1. Determination of the concentration at which Na-10 micellisation is initiated (i.e., the critical micelle concentration (cmc)) is not possible from this curve as there are no defined breaks. A consequence of the curve having a slowly changing slope is either that the system cannot be characterised by only free surfactant in water before the cmc and micelles plus free surfactant in water once the cmc is attained or that aggregation of the surfactant molecules is gradual with the aggregation number increasing with concentration. The first explanation (for the case of Na-10 where hydrolysis occurs in aqueous solution) is more likely to be the true situation. Hence other species must be present in solution which influence the aggregation of the surfactant.

The corresponding surface tension curve as measured by the du Noüy ring method at 25 °C is shown in Fig. 2.

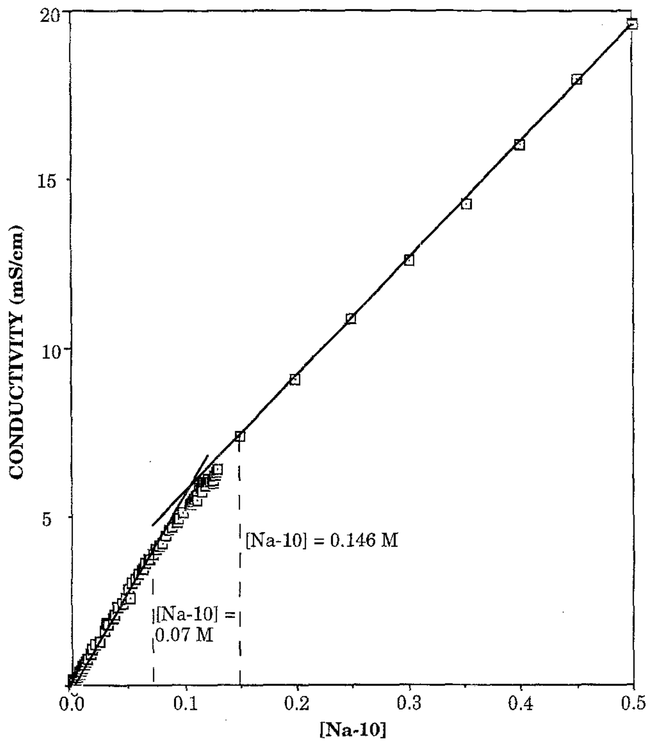

Fig. 1 Electrical conductivity of Na-10 in water measured at 25 °C. The two linear fits to the data show that for concentrations between ca. 0.07 and 0.15 M Na-10 (region indicated by the dotted lines) the conductivity is changing gradually with concentration and neither fit predicts the measured conductivity (i.e., there is no definitive break indicating the onset of micellisation). Errors are indicated by the size of the data points

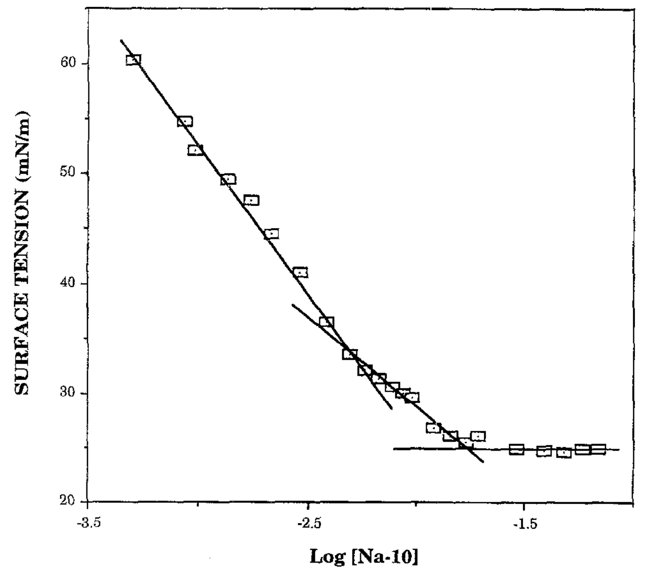

Fig. 2 Surface tension of Na-10 in water measured at 25 °C using the du Noüy ring method. Two breaks occur in the curve corresponding to Na-10 concentrations of ca. 5×10^{-3} and 0.02 M. Errors are indicated by the size of the data points

The surface tension curve shows three separate regions; two pseudo linear regions are observed before a plateau in the surface tension is reached. It is a mistake though to assume that this plateau is due to the solution undergoing aggregation to form micelles (yielding the true cmc) as is usually presumed in surface tension experiments. The observance of two almost linear regions prior to the plateau in the surface tension curve indicates the presence of auxiliary components in solution, which affect the solution behaviour and hence the concentration at which the surface tension plateaus out. The two breaks in the surface tension plot correspond to Na-10 concentrations of ca. 5×10^{-3} and 0.02 M. Note that the plateau observed here may be due to a solubility limit having been reached.

Conductivity and surface tension measurements (which involve the air/water interface) have been shown [25, 26] to be extremely sensitive to changes in the pH of the solution. Measurement of the surface tension of aqueous solutions of fatty acid soaps (which like all salts of weak acids undergo hydrolysis) will therefore be affected by the hydrolysis of the soap since, the colloidal nature of the soap solutions is dependent upon the extent of hydrolysis [4, 27–37] which will also affect the conductivity of the solution. The pH of these solutions will therefore vary considerably with composition. Hence, determination of the cmc of fatty acid soaps using surface tension or conductivity methods is complicated. This will also be the case for other techniques if the change in the exact nature of the solution and the affect of changing solution pH is not taken into consideration.

It has been shown [29] that the presence of a fixed amount of NaOH suppresses hydrolysis of the soap enabling well defined cmc values to be obtained from both conductivity and surface tension experiments.

Another way of determining the solution behaviour of fatty acid soaps (and hence their cmc) at low concentrations is to monitor the solutions pH with increase in soap concentration. Solutions which do not undergo hydrolysis will, in agreement with the Debye–Hückel limiting law for uni-univalent electrolytes give a slope of $+1/2$ in the pH versus log [soap] curve indicating that the soap behaves as the salt of a strong base and a weak acid. As the concentration is increased, though marked deviations from ideal behaviour are often observed, another process is occurring which is becoming increasingly important in determining the solution behaviour. In the case of a fatty acid soap this process is hydrolysis, as already indicated from the surface tension and conductivity measurements.

Upon hydrolysis the parent fatty acid (HZ, where Z is the carboxylate ion) is formed which is able to exist as either free acid or as an acid soap (MHZ_2, where M is the counterion). The configuration of this acid soap dimer is assumed to be one in which the head groups are at opposite ends of the dimer and there is considerable overlap of the hydrocarbon chains [31, 32]. Note that this configuration is more stable and therefore forms in preference to the configuration where both head groups are located at the same end of the dimer due to head group repulsion and thermal effects. Hence, in solution it is assumed that hydrolysis of fatty acid soaps may be explained by the precipitation of only three solid phases, each having well defined composition: HZ, MHZ_2 and MZ (neutral soap). It should be noted that the term solid phase does not indicate the formation of a solid which will precipitate from solution under the conditions employed here but rather that this neutral species will separate out under appropriate experimental conditions (e.g. on decreasing temperature to reach the solubility limit). Any one of these three solid phases may be precipitated first on increasing the soap composition and at higher concentrations two solid phases may coexist (note that the combination HZ and MZ is unstable with respect to MHZ_2) [36].

It has been proposed [36] that which species is present in solution may be determined from the slope of the pH versus log [soap] curve and in this way the solution behaviour in the dilute concentration regime may be explained for fatty acid soaps in aqueous solution.

Figure 3 shows the pH versus log [Na-10] curve obtained at 25 °C. The curve shows four unique regions. At low concentrations (below ca. 0.02 M, corresponding to the second break observed in the surface tension curve) Na-10 acts as an electrolyte yielding the predicted slope of $+1/2$. Deviations from this slope in this concentration region may be due to the influence of carbon dioxide or small deviations from the exact soap concentration. Note that the largest deviations occur for concentrations of Na-10 below approximately 5×10^{-3} M which corresponds to the first break observed in the Na-10 surface tension curve. As the concentration of Na-10 is increased above 0.02 M the slope tends to $+1$, which is characteristic of the presence of HZ in solution. A gradual transition to a slope of $+3$ occurs at higher compositions indicative of MHZ_2 being present in solution. Note that this concentration range, over which the largest variation in the solution pH is observed, corresponds to the region in the Na-10 conductivity curve where the conductivity deviates from linearity (i.e., Na-10 concentrations between ca. 0.07 and 0.15 M). Therefore in this concentration range the conductivity of the solution will be most strongly influenced by the large increase in the solution pH. At higher concentrations the curve begins to flatten out, indicating the presence of MZ and finally becomes slightly negative, which suggests micelle formation [36]. See Lucassen [36] for a full account of hydrolysis in soap solutions as monitored by the pH of the solution. Hence, for the Na-10/water system the cmc may be determined from the maximum in the pH versus log [Na-10] curve and is ca. 0.4 M. Therefore the equilibrium processes occurring on increase in Na-10 concentration are

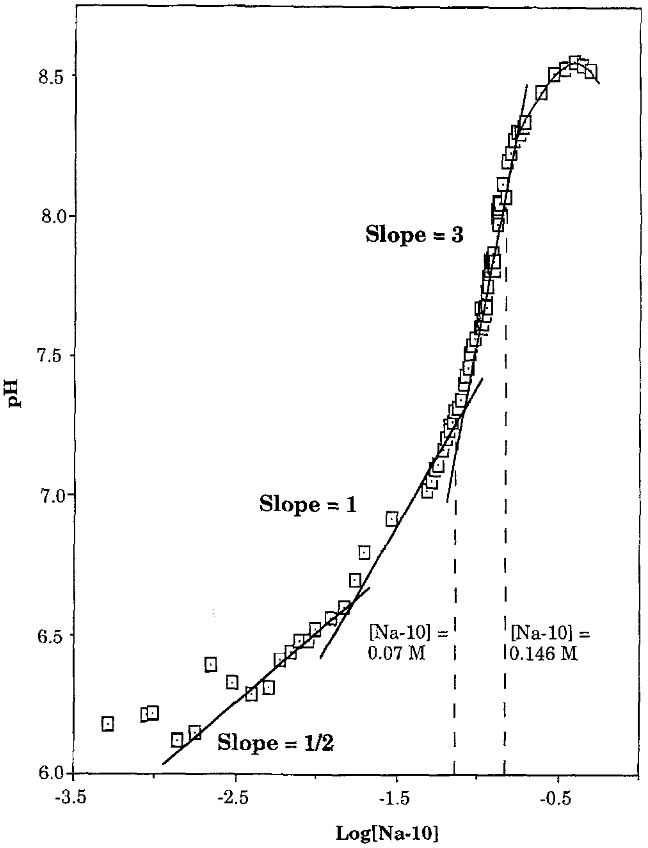

Fig. 3 Solution pH of aqueous Na-10 measured at 25 °C. A slope of $+1/2$ indicates that no precipitate is present and the solution acts as a dilute electrolyte solution. At higher concentrations the solid phase HZ is present which is characterised by a slope of $+1$. Formation of MHZ_2 manifests itself as a change of slope to $+3$. According to Lucassen [36] the cmc is detected by the occurrence of a slightly negative slope. The dotted lines indicate the concentration range shown in the Na-10 conductivity curve (Fig. 2). Errors in the experimental data points are indicated by the size of the points

$$\mathrm{NaZ} \overset{H_2O}{\rightleftharpoons} \mathrm{Z}^- + \mathrm{Na}^+ \overset{H_2O}{\rightleftharpoons} \mathrm{HZ} + \mathrm{OH}^- \overset{\mathrm{NaZ}}{\rightleftharpoons} \mathrm{NaHZ_2} \overset{\mathrm{NaZ}}{\rightleftharpoons}$$

$$\mathrm{NaZ} \overset{\mathrm{NaZ}}{\rightleftharpoons} (\mathrm{NaZ})_n$$

where the first process to occur is dissociation of the neutral soap producing the carboxylate ion, this then reacts with water to form the parent fatty acid. Further reaction with neutral soap yields the acid soap dimer. As the concentration of Na-10 is increased the predominant species in solution becomes the neutral soap which finally begins to aggregate to form micelles at the critical micelle concentration.

Hence the pH versus log [Na-10] curve confirms that in the Na-10/water system at low surfactant concentrations Na-10 undergoes considerable hydrolysis which dominates the solution behaviour.

The results obtained here for the dilute concentration regime of the Na-10/water system contrast those obtained by several other groups [5, 38–41]. The cmc for Na-10 has been reported to be either ca. 0.04 $\mathrm{mol \cdot kg^{-1}}$ [38, 39] or ca. 0.12 $\mathrm{mol \cdot kg^{-1}}$ [5, 40, 41] as determined by specific conductivity, fluorescence quenching and vapour pressure osmometry. The first reported cmc (0.04 $\mathrm{mol \cdot kg^{-1}}$) measured by Larrabee Jr et al. [38] from specific conductivity was later reported as being due to premicellisation of the Na-10 surfactant molecules and that the cmc was ca. 0.12 $\mathrm{mol \cdot kg^{-1}}$, it was also stated that hydrolysis accounted for an error of less than 0.1% [5]. Paleos et al. [39] also obtained a value for the cmc to be approximately 0.04 $\mathrm{mol \cdot kg^{-1}}$ using fluorescence quenching.

Monomeric self-assembly

For the binary system Na-10 in water, only two liquid crystalline phases are formed between 0 and 100 °C. A normal hexagonal phase (H_α, two-dimensional structure of hexagonal symmetry with liquid-like chains) forms between 42.6% and 55.5% by weight and a lamellar gel phase (L_δ, layered structure with frozen chains in a helical conformation) between 69.8% and 80.8% at 25 °C. Between 55.5 and 69.8% the two phases coexist. The partial phase diagram for this system as determined in this study is shown in Fig. 4. The full phase behaviour for this system has been described previously, see ref. [1].

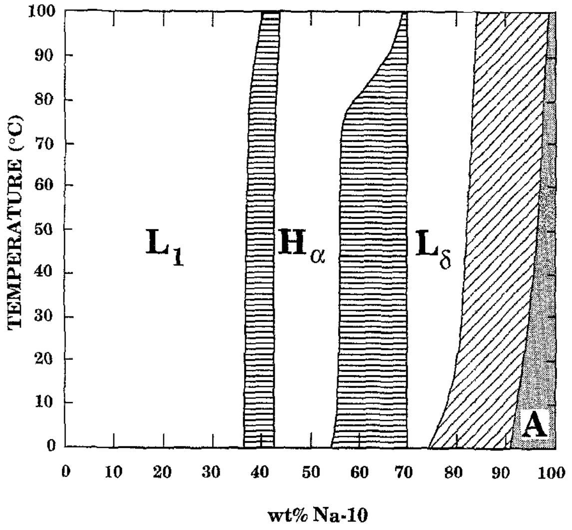

Fig. 4 Schematic binary phase diagram of the Na-10/water system [1]. L_1: micellar solution, H_α: normal hexagonal phase, L_δ: lamellar gel phase with frozen hydrocarbon chains in a helical conformation perpendicular to the plane of the bilayers, and A: hydrated Na-10 crystals. The horizontally shaded area indicated a region where two liquid crystalline phases coexist (tie lines) and the diagonally shaded area where L_δ coexists with hydrated crystals of Na-10

Polymeric Na-10

Polymerisation of the monomeric form of Na-10 was not possible due to the insolubility of this surfactant in most solvents. Hence, the parent fatty acid (undecenoic acid) of Na-10 was polymerised in a chloroform solution (0.25 M) via thermal initiation of added α, α'-Azobis(isobutyronitrile) (AIBN, $\mathrm{(CH_3)_2C(CN)N{=}N(CN)C(CH_3)_2}$, 10 mol% to surfactant). The reaction mixture was maintained at 60 °C for 7 days after which the polymerisation had preceded to approximately 80%. Increasing the reaction time did not increase the extent of polymerisation significantly. The corresponding sodium salt polymer (i.e., polymeric Na-10) was obtained by reacting the acid polymer with an equimolar aqueous solution of NaOH. The resulting precipitate was washed with ethanol, dissolved in water and then freeze dried. Pure polymeric Na-10 was obtained by removal of the monomer and oligomer units using Sephadex G-15 a size exclusion gel filtration packing material, having a molecular weight cut-off of 1500, corresponding to oligomers up to seven monomer units long. It must be noted that this method of preparation produces polymers which are polydisperse and therefore the polymeric Na-10/water system cannot be regarded strictly as a binary system.

NMR Analysis (analysed for head-to-tail configuration only): Proton $\mathrm{(C\underline{H}_2)_4{-}(CH_2)_2{-}C{=}O}$ 1.32 δ; $\mathrm{C\underline{H}_2{-}(CH_2)_6{-}C{=}O}$ 1.52 δ; $\mathrm{C\underline{H}}$ 1.62 δ; $\mathrm{C\underline{H}_2{-}CH_2{-}C{=}O}$ 1.75 δ; $\mathrm{C\underline{H}_2{-}C{=}O}$ 2.13 δ; $\mathrm{(C\underline{H}_2)_2{-}CH}$ 5.01 δ; $\mathrm{C\underline{H}_2{-}(CH_2)_7{-}C{=}O}$ 2.67 δ. Carbon 13 $\mathrm{\underline{C}H_2{-}C{=}O}$ 26.07 δ; $\mathrm{(\underline{C}H_2)_2{-}CH}$ 27.66 δ; $\mathrm{\underline{C}H_2{-}CH_2{-}C{=}O}$ 28.97 δ; $\mathrm{(\underline{C}H_2)_5{-}(CH_2)_2{-}C{=}O}$ 29.06 δ; $\mathrm{\underline{C}H_2{-}(CH_2)_7{-}C{=}O}$ 37.50 δ; $\mathrm{\underline{C}H}$ 54.38 δ; $\mathrm{\underline{C}{=}O}$ 182.44 δ (compare with monomer discussed earlier).

In contrast to the phase behaviour of the monomeric form of Na-10 in water, polymeric Na-10 forms only one liquid crystalline phase between 20 ° and 100 °C. A lamellar phase forms between 60.5 and 69.7 wt% of polymeric Na-10 at 20 °C. At concentrations below 45.4 wt% a micellar phase forms. Between 45.4 and 60.5 wt% the two phases coexist. Figure 5 shows the partial phase diagram for the polymeric Na-10/water system.

The polymeric Na-10 lamellar phase displays several different optical textures when viewed through crossed polarizing filters. Figure 6 shows a typical "mosaic" texture which contrasts the "oily streak" texture shown in Fig. 7. Both textures are typical of those commonly observed for lamellar liquid crystalline phases and are

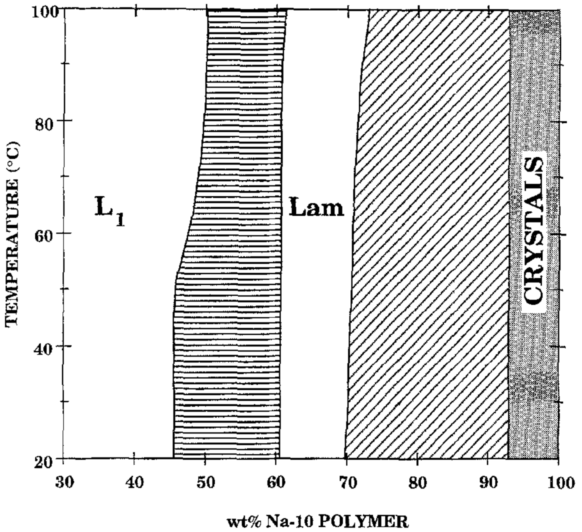

Fig. 5 Partial phase diagram for the polymeric Na-10/water system. L_1: micellar solution, Lam: lamellar phase, and crystals: hydrated polymer crystals. The horizontally shaded area indicates a region of coexistence between the micellar and lamellar phases (where the lines indicate tie lines between the two phases). The diagonally shaded area indicates coexistence between the lamellar phase and hydrated polymer crystals

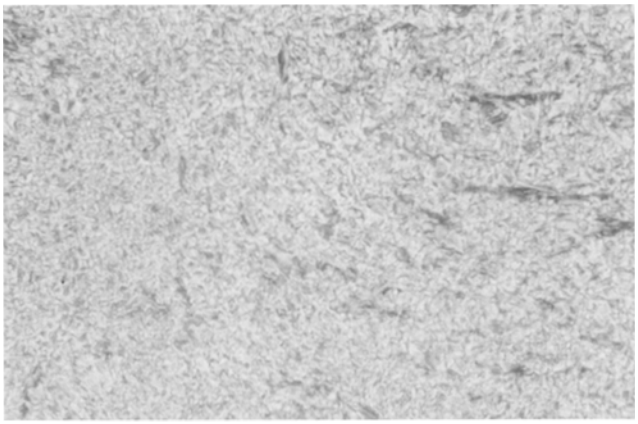

Fig. 6 Mosaic texture observed for the polymeric Na-10 lamellar phase (crossed polarising filters, magnification 240), where the layers of the phase are parallel to the glass slide, (68.7 wt%, 86.7 °C)

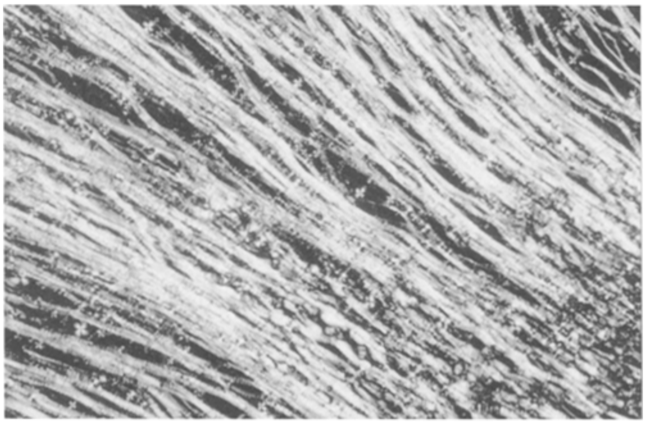

Fig. 7 Oily streak texture obtained for the polymeric Na-10 lamellar phase (crossed polarising filters, magnification 240), where the layers are parallel to the glass slide, (68.7 wt%, 75.5 °C)

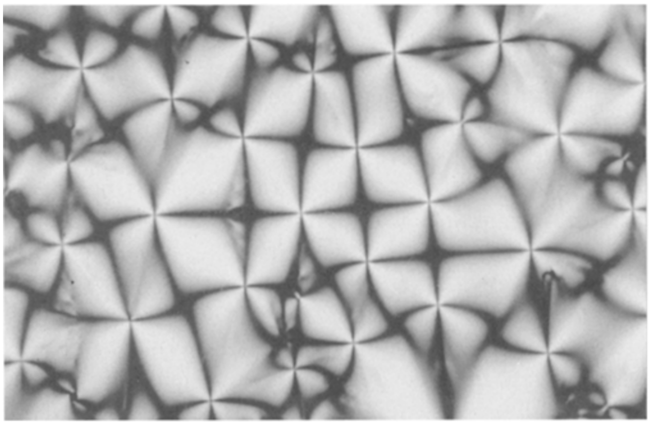

Fig. 8 Optical texture observed for the lamellar phase of polymeric Na-10 (crossed polarising filters, magnification 480). Note the presence of both positive and negative spherulites and the "pin wheel" effect displayed by the negative as compared with the positive spherulites which maintain a perfect cross at their core on rotation of the polariser and analyser, (60.7 wt%, 25 °C)

characteristic of a homeotropic orientation (i.e., the orientation in which the optic axis is normal to the plane of the preparation) [42–46].

Figure 8 shows a third optical texture also commonly observed in the polymeric Na-10 lamellar phase. Here both positive (where the radial direction is "slow") and negative (where the radial direction is "fast") spherulites (in the vein of Rosevear [42]) are apparent. The positive and negative spherulites are determined by considering the extinction cross as if it were uniaxial interference figure, hence positive corresponds to a radial and negative to a tangential vibration direction for the component of higher refractive index. The positive spherulites are characterised by extinction arms which are narrowest at the centre of the cross whereas the negative spherulites are broadest at the intersection. Each positive spherulite constitutes a focal domain viewed normal to its elliptical base. From this figure it may be seen that the positive spherulites (observed due to the presence of line defects of strength $s = \pm 1$ in the sample) are such that the extinction cross formed by the brushes remains oriented perpendicular to each other upon rotation of the polariser and analyser. This is not the case for the negative spherulites, where the plus shape of the spherulite is distorted upon rotation.

This distortion is due to the arms of the negative spherulite being at different levels. That is, the negative spherulite results from the vertices of the adjacent positive spherulites which are alternatively on the top and bottom surfaces of the preparation [42]. This texture is, therefore also characteristic of a lamellar liquid crystalline phase (since negative spherulites are not observed for other phases). It should be noted that while both positive and negative spherulites are often observed in optical textures formed by lamellar liquid crystalline phases (both being apparent in the oily streak texture shown in Fig. 7) the uniform matrix formed by alternative positive and negative spherulites shown here has not been previously observed such that both $s = +1$ and $s = -1$ line disclinations are randomly distributed throughout the sample at a single focus point. A similar texture, without these features, has been observed in a thermotropic smectic liquid crystal [47] and lamellar lyotropic liquid crystalline phases of some lipid/water systems [48] which have been described as forming due to the presence of a network of parabolic focal conics. This network can be used to explain some of the features observed in the texture produced by the polymeric Na-10 lamellar phase but does not describe the texture fully. Formation of this texture may therefore, in addition to the parabolic focal conic network, be due to unusual anchoring of the bilayers to the substrate and/or the orientations adopted by the bilayers of the phase due to the presence of polydisperse polymer, i.e., the ordering of the phase.

All three optical textures of the polymeric Na-10 lamellar phase were observed for both bulk samples and concentration gradients performed at various temperatures.

The structure of this phase was established by small-angle x-ray scattering (SAXS). The diffraction pattern of the polymeric Na-10 lamellar phase is characterised by up to three sharp rings in the ratios of 1:2:3 as expected for parallel planes and one diffuse ring at wide-angles ($Q = 1.4$ Å^{-1}) indicative of liquid-like chains. No other rings were observed. Calculation of the interplanar spacing from the primary Bragg reflexion yields a repeat distance of the order of 35 Å. This value is consistent with that obtained for the Na-10 lamellar gel phase (where $d \approx 30$ Å[1]) such that the hydrocarbon chains are no longer in a frozen state and helical conformation (i.e., the expansion of the unit cell length is consistent with the ratio of 1.145 determined by Tardieu et al. [22]). Head group areas are also consistent with a bilayer structure. Calculated structural parameters are given in Table 1 and were determined assuming that the specific volume of polymeric Na-10 is the same as that for monomeric Na-10 when the chains are in the alpha configuration [1]. This assumption should not introduce significant errors into the calculated structural parameters. All equations were calculated for $T = 27$ °C, and based on an assumed structure of planar flat bilayers.

Comparison of the monomeric and polymeric Na-10/water systems shows that, in the concentrated region few similarities occur between the two. This indicates that the nature of the hydrocarbon chain plays a critical role in determining the self-assembly of these systems. This lack of overlapping regions between the two systems has the consequence that polymerisation of the liquid crystalline phases of Na-10 may not involve retention of the underlying surfactant mesophase. This is particularly true in the case of the lamellar gel phase where the nature of the paraffinic chains differs from that in the other regions of the phase diagram. Here, not only is the carbon–carbon double bond lost upon polymerisation but it is likely that the frozen helical conformation of the paraffinic chains is not maintained either. The hexagonal and micellar phases should not be influenced to the same extent and hence a different behaviour should be observed for these two

Table 1 Structural parameters calculated for the lamellar phase of polymeric Na-10 at 27 °C

Polymeric Na-10% (w/w)	Phase	Observed Q (Å^{-1})	Unit cell length (a) (Å)	Volume fraction Φ	Surfactant aggregate thickness (d_s) (Å)	Water thickness (d_w) (Å)	Mean area per polar head (A) (Å^2)	hkl
54.2	L_1	0.132	–	0.41	–	–	–	–
	+							
	Lam	0.196	32.1	0.56	17.9	14.2	31.6	001
		0.390						002
		0.580						003
62.7	Lam	0.193	32.5	0.58	18.9	13.7	29.9	001
		0.385						002
		0.575						003
67.0	Lam	0.188	33.4	0.63	20.9	12.5	27.0	001
		0.375						002
68.4	Lam	0.186	33.9	0.64	21.7	12.2	26.0	001
		0.370						002

phases as compared with the lamellar gel phase upon polymerisation.

Polymerisation of liquid crystalline phases

Four regions in the Na-10/water system were chosen as being representative for polymerisation in the assembled forms of Na-10; the dilute and concentrated regions of the micellar phase (5 and 30 wt% Na-10), the hexagonal phase (50 wt% Na-10) and the lamellar gel phase (75 wt% Na-10). The surfactant was not observed to self-initiate during equilibration.

Table 2 shows the percentage conversions for the four regions of the Na-10/water system activated by thermal initiation of added AIBN (10 mol% to surfactant) at 60 °C or by photochemical initiation. Note that an error of approximately ±5% can be expected in these values due to inaccuracies in the measured integration values obtained from proton NMR.

Both types of initiation were found to yield similar results. Thermal initiation of the dilute micellar solution though appears to involve a gradual increase in the rate of polymerisation with time. A plateau being reached after approximately 2 or 3 days. This initial increase was not observed for any of the other compositions (initiated either thermally or photochemically) which reached their final conversion rapidly.

Table 3 presents the calculated mean and median for the polymerisation in the different regions. Results indicate that, for all Na-10 compositions, polymerisation via thermal initiation is more successful. Polymerisation in the liquid crystalline phases of Na-10 is dramatically reduced as compared with that in isotropic solution which was found to polymerise to approximately 80%. That is self-assembly of the Na-10 monomer acts to inhibit polymerisation of the surfactant.

Final samples were polymerised via thermal initiation (10 mol% AIBN to surfactant) at 60 °C for a period of 2 days. Both the micellar and hexagonal phases remained visibly unchanged, whereas the lamellar gel phase underwent a phase transition upon polymerisation.

The partially polymerised micellar solutions (25.8 and 21.3 percent conversion, respectively) when viewed under

Table 2 Percentage conversions for the four regions of the Na-10/water phase diagram polymerised either thermally or photochemically

Type of initiation	Time (days)	Dilute micellar phase	Concentrated micellar phase	Hexagonal phase	Lamellar gel phase
Thermal initiation	0.5	0.0	0.0	1.3	19.0
	1.0	10.5	19.6	32.3	13.0
	2.0	12.7	18.0	20.8	23.4
	3.0	30.0	28.0	–	–
	4.0	19.5	9.0	22.8	16.8
	6.0	15.0	14.6	14.6	19.6
	7.0	38.5	24.8	44.4	–
	8.0	–	–	–	24.0
	9.0	–	15.4	19.7	–
	10.17	41.9	47.0	56.0	–
	12.0	50.3	24.1	21.4	–
	15.0	–	23.2	34.5	18.1
	20.0	38.5	29.2	16.5	–
	24.0	36.6	29.5	–	–
	–				
Photochemicalinitiation	0.25	44.5	24.7	11.9	6.6
	0.5	26.7	17.2	13.1	7.1
	0.75	24.5	24.1	8.8	19.2
	0.83	20.9	8.5	14.5	17.7
	1.0	21.5	40.7	13.5	10.4
	2.0	16.1	14.0	12.5	11.9
	3.5	8.0	23.3	15.6	2.0
	4.0	22.6	18.0	12.6	9.9
	5.5	15.4	36.6	13.4	18.1
	6.0	32.2	25.3	20.6	14.0
	8.0	20.9	9.8	7.7	13.7
	8.75	23.9	12.8	19.6	15.6
	10.0	21.6	13.4	8.4	11.8
	12.0	27.4	13.4	13.6	13.6
	14.0	14.2	18.2	10.6	10.1
	20.0	36.8	19.9	15.5	11.3

Table 3 Statistics of the extent of polymerisation for the four Na-10 liquid crystalline phases

		Low weight percent micellar solution	High weight percent micellar solution	Hexagonal phase	Lamellar gel phase
Thermal initiation	median	30.0	23.2	21.4	19.0
	mean	26.7	21.7	25.8	19.1
	standard deviation	15.2	10.9	14.4	3.5
Photochemical initiation	median	23.3	19.0	13.3	11.9
	mean	23.6	20.0	13.2	12.1
	standard deviation	8.6	8.7	3.5	4.4

crossed polarising filters were optically isotropic. The molecular weight of both samples was determined to be less than 8000 (corresponding to approximately forty monomer units) via dialysis. Although this could indicate intramicellar polymerisation it is unlikely as the molecular weight of polymeric Na-10 was also found to be less than 8000. This suggests that free radical initiation of the allyl polymerisable moiety in this position does not result in large molecular weight polymers. This is directly comparable with the results obtained for ω-UTAB where the molecular weight of the polymers synthesised from both isotropic and self-assembled states were also below 8000 [3]. It should be noted that while the aggregation number of the micelles may be less than 40 at low surfactant concentrations it is likely to increase dramatically with increase in concentration. This being due to elongation of the aggregates as evidenced by the formation of a hexagonal phase subsequent to the micellar phase. That is, in the dilute region of the micellar phase a single polymer chain may constitute a micellar aggregate but this is unlikely in the more highly concentrated regions where the polymer will be only one component of the aggregate.

The optical texture observed for the partially polymerised Na-10 hexagonal phase (15.7 percent conversion) is shown in Fig. 9 and is typical for lyotropic hexagonal phases. Note that several edge dislocations can be distinguished and striations, as analysed by Rogers and Winsor [49], are also evident. The hexagonal phase was found to be stable to 100 °C. Hence the stability of the partially polymerised phase is comparable with that of the pure monomeric hexagonal phase.

The lamellar gel phase (20.7 percent conversion) unlike the micellar and hexagonal phases undergoes a phase transition and separation upon polymerisation. Figures 10 and 11 show the presence of three phases in a given sample. Upon polymerisation the original lamellar gel phase transforms yielding a hexagonal phase, a lamellar phase and hydrated crystals. Figure 10 shows the textures due to the lamellar gel and hexagonal phases and Fig. 11 that of the lamellar phase.

Fig. 9 Optical texture observed for the partially polymerised Na-10 hexagonal phase (crossed polarising filters, magnification 240). Note the presence of edge dislocations and striations, (49.3 wt% Na-10, 98.3 °C)

All four components remain present on increasing the temperature to 100 °C. It was not possible to physically separate any of these four components so as to analyse each separately and determine which phases are comprised of polymeric Na-10. A plausible explanation, however, can be based on the phase diagrams of the pure monomeric and polymeric forms of Na-10 (Figs. 4 and 5, respectively). Polymerisation of the lamellar gel phase induces a phase transition to a lamellar phase. Specifically the paraffinic chains which were originally frozen and in a helical conformation become more liquid-like and are no longer in the helical conformation. From the polymeric phase diagram, at a polymeric Na-10 composition of approximately 75% by weight the lamellar phase coexists with hydrated polymer crystals. This therefore may explain the presence of the lamellar phase and hydrated crystals in the partially polymerised lamellar gel phase. A consequence of this phase separation of the polymerised form of Na-10 is that the remaining unpolymerised sample has an overall composition less than 75 wt% Na-10. From the monomeric phase diagram, this would push the system into the two

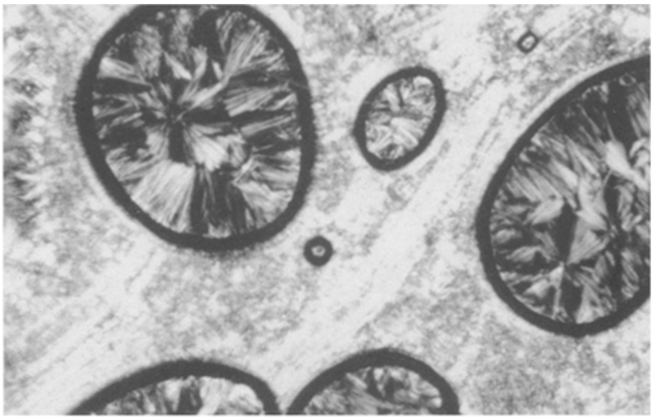

Fig. 10 Optical textures observed for the hexagonal and lamellar gel phases of the partially polymerised Na-10 lamellar gel phase (crossed polarising filters, magnification 240)

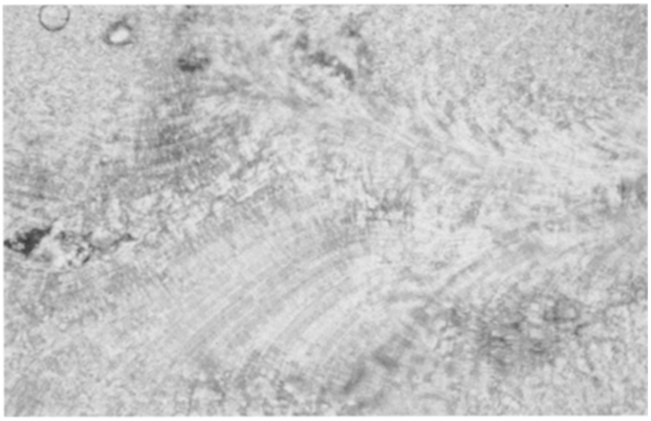

Fig. 11 Lamellar texture observed in a sample of the partially polymerised Na-10 lamellar gel phase (crossed polarising filters, magnification 240)

phase region between the hexagonal and lamellar gel phases. Hence the presence of all four components may be explained if it is assumed that the hexagonal and lamellar gel phases contain no polymerised Na-10 and that the polymerised form yields a lamellar phase and hydrated polymer crystals.

To substantiate the findings of the optical microscopy investigations (i.e., that the micellar and hexagonal phases remain unchanged and that the lamellar gel phase separates upon polymerisation) SAXS experiments were performed on the partially polymerised samples.

The concentrated partially polymerised micellar phase produced a diffraction pattern at small- and wide-angles consisting of one diffuse ring only. The average distance between the aggregates (Table 4) is comparable to that observed for the pure monomeric micellar phase where $Q \approx 0.164\,\text{Å}^{-1}$ [1]. This indicates that the nature of the micellar solution remains largely unperturbed upon polymerisation.

Similarly, the diffraction pattern at small-angles for the partially polymerised hexagonal phase consisted of four sharp Bragg peaks in the ratios of $1:\sqrt{3}:\sqrt{4}:\sqrt{7}$. No other peaks were observed. At wide-angles only one diffuse ring was present at $Q = 1.4\,\text{Å}^{-1}$ indicating liquid-like chains [50]. These results in conjunction with those from optical microscopy indicate that upon partial polymerisation the underlying geometry of the surfactant molecules is maintained in the original hexagonal phase. Calculation of the structural parameters for this resultant phase show that there is a contraction in the unit cell length and an increase in the head group area (Table 4). These values are observed to change from ~45 Å and ~35 Å^2 for a monomeric sample to ~37 Å and ~44 Å^2 in the partially polymerised sample, respectively). This is expected due to an increased confinement of the surfactant molecules due to the presence of polymer.

The diffraction pattern at small-angles obtained for the partially polymerised lamellar gel phase was very complicated, consisting of several Debye–Scherrer rings. Using the information obtained from optical microscopy, the pattern was able to be indexed as follows. The presence of the hexagonal phase was evidenced by four sharp rings in the ratios of $1:\sqrt{3}:\sqrt{4}:\sqrt{7}$. The lamellar phase gave two sharp rings in a ratio of 1:2 and the lamellar gel produced four sharp Bragg peaks having ratios of 1:2:3:4 and a diffuse central ring located as $0.117\,\text{Å}^{-1}$ (Table 4). This diffuse scattering reflects the existence of correlations over a range of 53.7 Å. At wide-angles a diffuse ring at $Q = 1.4\,\text{Å}^{-1}$ was detected which was attributed to the hexagonal and lamellar phases. In conjunction with this ring two sharp reflexions at $Q_1 = 1.31\,\text{Å}^{-1}$ (strong) and at $\sqrt{2}Q_1$ (weak) and two diffuse rings at $Q_0 = 0.92\,\text{Å}^{-1}$ and at $2Q_0$ were observed and were due to the presence of the lamellar gel phase of type L_δ [1, 22].

Table 4 gives a summary of these results. The structural parameters for the different phases arising from the lamellar gel phase could not be determined since the volume fraction for each phase was uncertain. The calculated unit cell lengths for each phase do though correspond reasonably well to those determined for the pure monomeric phases [1]. The structural parameters for the hexagonal phase were calculated assuming that the composition remains unchanged upon polymerisation (i.e., the phase is retained and no phase separation or transition has occurred). The specific volume of the surfactant was also assumed to vary little upon polymerisation. All equations were calculated for $T = 27\,^\circ\text{C}$.

These results indicate therefore that the micellar and hexagonal phases remain largely undisturbed upon partial

Table 4 Structural parameters for the partially polymerised surfactant mesophases of Na-10 at 27 °C

Na-10 % (w/w)	Phase	Observed Q (Å^{-1})	Unit cell length (a) (Å)	Volume fraction Φ	Surfactant aggregate thickness (d_s) (Å)	Water thickness (d_w) (Å)	Mean area per polar head (A) (Å^2)	hkl
30.1	L_1	0.168	–	0.26	–	–	–	–
49.3	H_α	0.198	36.6	0.44	25.6	11.0	44.1	$10\bar{1}0$
		0.345						$11\bar{2}0$
		0.395						$20\bar{2}0$
		0.521						$21\bar{3}0$
73.9	H_α	0.193	37.6	–^{a}	–	–	–	$10\bar{1}0$
		0.335						$11\bar{2}0$
		0.388						$20\bar{2}0$
	plus	0.511						$21\bar{3}0$
	L_α	0.209	30.1	–^{a}	–	–	–	001
	plus	0.419						002
	L_δ	0.117*						
		0.221	28.4	–^{a}	–	–	–	001
		0.441						002
		0.657						003
		0.870						004

* Diffuse inner ring.

[a] The correct weight percentage for each of these phases is unknown due to phase separation. Hence, the structural parameters for these phases could not be evaluated.

polymerisation with the only changes being manifested as a slight change in the calculated structural parameters. In contrast the lamellar gel phase undergoes a phase transition and separation upon polymerisation.

Discussion

The change from a quaternary ammonium head group to a fatty acid soap has been shown to have a significant effect on the solution behaviour of the surfactant in the dilute concentration regime. Na-10 undergoes hydrolysis in this region which promotes the formation of the parent acid and acid soap dimers prior to micellisation. The formation of the parent fatty acid and dimers is used to explain the results obtained from measurements of the solution's conductivity, surface tension and pH. The formation of acid dimers has also been used to explain deviations in the measured physical parameters of aqueous solutions of monoalkyl sulfates [32, 34, 51, 52]. The creation of the acid soap dimers sufficiently stabilises the surfactant in aqueous solution such that the initiation of surfactant aggregation to form micelles is shifted to higher surfactant concentrations. It should be noted that the effective chain length of Na-10 is equivalent to a C_8 or C_9 hydrocarbon chain only which will therefore, also act to shift the cmc to higher concentrations of Na-10 [53]. Therefore, the combination of a fatty acid head group and a shortened paraffinic chain can be used to explain the high cmc observed for Na-10 in aqueous solution. Comparison with the equivalent non-polymerisable fatty acid soaps sodium octanoate and sodium decanoate (the C_7 and C_9 equivalents) which have cmcs at 25 °C of ca. 0.35 and 0.1 M, respectively [35] shows that this combination does indeed push the cmc to higher concentrations. Note that these values have been determined from conductivity measurements which were corrected for hydrolysis [54]. The presence of the terminal double bond, as in the case of ω-UTAB [3] also acts to further increase the concentration at which aggregation occurs as compared with the non-polymerisable analogue [55].

The phase behaviour observed for the monomeric Na-10/water system does not resemble that observed for any of the quaternary ammonium systems presented previously [2, 3]. The balance of interactions has been severely altered by replacement of the quaternary ammonium head group and the shortening of the hydrocarbon chain. The phase progression displayed by the Na-10/water system is therefore difficult to compare with that observed for the systems previously discussed. Some similarities can however be drawn between Na-10 and ω-UTAB [3]. Both surfactants have been shown to have an increased intrinsic rigidity of the paraffinic chains which acts to decrease the solubility of the surfactant and promote ordering of the chains upon aggregation. This preference to form more highly ordered systems being substantially enhanced in the Na-10/water system. Any further correlation is not possible since the introduction of the fatty acid head group cannot be isolated from the consequential reduction in the paraffinic chain length and hence the greater dominance of the terminal carbon–carbon double bond. But it is apparent that this combination affects significantly the surfactants solution behaviour and will also have important contributions to the observed behaviour upon polymerisation.

Polymerisation of Na-10 prior to self-assembly was achieved to a similar extent as was the case for ω-UTAB (i.e., the polymerisations went to near completion) [3]. This indicates that the nature of the head group has little effect on the polymerisation mechanism when the carbon–carbon double bond is sufficiently isolated from it. Hence it may be assumed that the polymerisation of Na-10 is attained in an identical manner to that of ω-UTAB and that the so formed polymers will vary only in their different head groups and paraffinic chain lengths. It has been shown earlier that polymerisation prior to self-assembly precludes the formation of both the hexagonal and lamellar gel phases which were formed in the Na-10/water system. In contrast, the polymeric form of ω-UTAB has a similar phase progression to that observed for the monomer differing only in the temperatures and compositions at which the different mesophases are formed [3]. This difference in the behaviour of the two polymeric forms must therefore be explained by the change in head groups of the original surfactants. The average head group area of the trimethylammonium bromide group is considerably larger than that of the sodium carboxylate, whereas the paraffinic chain backbone of the polymers will be almost identical. The intrinsic shape of the Na-10 polymer, in comparison to polymeric ω-UTAB will therefore be more commensurate with the formation of the bilayer structure of the lamellar phase rather than the more highly curved geometries required for formation of the hexagonal and cubic phases. This indicates that the micellar phase formed by polymeric Na-10 is most likely comprised of disk-shaped aggregates.

However, this explanation cannot be used to explain why a hexagonal and lamellar gel phase are formed by the monomer and not by the polymeric form of Na-10. This difference, in contrast to the explanation given above is due to the change in the nature of the paraffinic chains. The lamellar gel phase is not able to be formed in the polymeric Na-10/water system since formation of the polymer precludes adoption of a helical configuration by the paraffinic chains. The alternative to this is therefore to form a lamellar phase. In contrast to this explanation, formation of the hexagonal phase by monomeric Na-10 may be due to the increased flexibility and mobility available to the paraffinic chains in the non-polymerised form. This increased freedom is such that curved geometries are able to be formed prior to the orienting effect of the shortened paraffinic chain and the terminal carbon–carbon double bond become dominant and induce a disorder/order transition yielding the lamellar gel phase.

From the monomeric and polymeric Na-10/water phase diagrams the precise nature of the paraffinic chains is therefore critical in determining the self-assembly of the amphiphiles. This is carried over into the polymerisation of the liquid crystalline phases of Na-10. The micellar and hexagonal phases, where the paraffinic chains are in a fluid-like state are found to respond towards polymerisation in an identical manner to the micellar and hexagonal phases of ω-UTAB [3]. Specifically, the integrity of the mesophases remains unaltered upon partial polymerisation, although it is unlikely that intra-aggregate polymerisation has occurred. Again, as was the case for polymerisation in the liquid crystalline phases of ω-UTAB [3], the extent of polymerisation was found to be significantly reduced as compared to polymerisation of an isotropic solution of Na-10. This may be explained by the high degree of mobility of the paraffinic chains and the surfactant aggregate acting as a cage inhibiting the polymerisation (see reference [3] for a fuller explanation).

A considerable amount of work has been performed on polymerisation in the micellar and premicellar regions of the Na-10/water phase diagram [5, 24, 38–41, 56–60]. Varying results have been indicated by these different groups. Paleos et al. [39] assuming a cmc of ca. 0.04 M polymerised "micelles" in aqueous 0.1 M solutions (which according to the results obtained here corresponds to the concentration range where the acid dimer predominates) obtaining intra-micellar polymers using γ irradiation. A similar result was reported by Sprague et al. [5, 38, 40, 56, 60] who also used γ irradiation but assumed a cmc of 0.12 $\mathrm{mol \cdot kg^{-1}}$ (samples were polymerised above and below the stated cmc but none were above 0.4 M – the cmc determined here, again, this concentration range is dominated by the presence of the acid dimer). Polymerised samples both above and below 0.12 $\mathrm{mol \cdot kg^{-1}}$ yielded similar results when subjected to fluorescence quenching, viscosity, conductivity, and electron spin resonance experiments. Chu and Thomas [41] have also based their results on the conductivity measurements of Sprague et al. [5, 38, 40, 56, 60] (i.e., there is a change in the aggregation state at concentrations of approximately 0.04 and 0.12 $\mathrm{mol \cdot kg^{-1}}$) indicating that the molecular weight of the produced polymer was different in the region below 0.043 M and above 0.15 M due to an increase in the aggregation number of the micellar units. Polymerisation was performed either by γ irradiation or thermal initiation of added potassium persulphate (a water soluble initiator). Durairaj et al. [24, 57, 58] indicated that polymerisation occurred between 15 and 30% conversion only (which is similar to the results obtained here) when solutions in excess of 0.4 M Na-10 were polymerised thermally using ammonium presulphate (a water soluble initiator) as the added initiator. Finally Shibasaki and Fukuda [59] showed that polymerisation via γ irradiation in a 10 wt% micellar solution was only polymerised to approximately 10%.

Others [59, 61, 62] have also reported polymerisation in the hexagonal region of the Na-10/water system. Shibasaki and Fukuda [59], whose phase diagram determined by thermal analysis contrasts strikingly with that both obtained here and by Friberg et al. [61, 62] (who determined the phase boundaries of the hexagonal phase during their study of the polymerisation in the Na-10 hexagonal phase) indicated that polymerisation by γ irradiation in the Na-10 "hexagonal phase" occurred to a maximum of 30% conversion. It should be noted that the results obtained here and by Friberg et al. suggest that the region thought to be a hexagonal phase by Shibasaki and Fukuda is actually a concentrated micellar phase. These results, when this is taken into consideration, correlate well with the percentage conversion determined for the concentrated micellar phase in this study. No description of the state of the partially polymerised sample was given.

Friberg et al. [61, 62] have stated that polymerisation of the Na-10 hexagonal phase via thermal initiation of potassium persulphate is essentially complete in 1 day and is transformed into a lamellar phase. The resulting polymer was found to have a molecular weight of approximately 55 000, corresponding to approximately 270 monomer units. Therefore, the results of Friberg et al. differ in comparison with those obtained in this study, where polymerisation occurred to approximately 30% only and no phase transition was observed to occur. At this stage, a reason for this difference is unknown.

Polymerisation of the lamellar gel phase, where the chains are frozen and in a helical arrangement does not maintain the integrity of the phase. This disruption to the underlying surfactant geometry is caused by a loss of order in the paraffinic chains upon polymerisation. Here, also the extent of polymerisation was reduced when compared with an isotropic solution. An explanation for this reduction cannot be given in a manner similar to that for the micelle and hexagonal phases where the high degree of mobility was used. Here instead, the highly ordered conformation adopted by the paraffinic chains is used, which increases the average distance between the carbon–carbon double bonds. This increased distance and the inherent rigidity of the chains of the lamellar gel phase restricts the carbon–carbon double bond from adopting the correct orientation for polymerisation to proceed and the free radical is lost via recombination. Hence again the surfactant aggregate acts as a cage inhibiting polymerisation and here the extent of polymerisation is reduced to an even lower value than in the phases where the chains are in a molten state.

Shibasaki and Fukuda [59] have also reported polymerisation in a Na-10 gel phase. Again the composition of this phase does not correlate with the composition of the lamellar gel phase determined here. Polymerisation occurred to approximately 20% and no analysis of the resulting sample was given.

Therefore as was observed in the self-assembly of Na-10 in the monomeric versus polymeric forms the nature of the paraffinic chain is critical in determining the behaviour of the system.

Conclusions

The position of the carbon–carbon double bond at the end of the paraffinic chain has been found to facilitate polymerisation in non-aggregated solutions as compared with polymerisation in the head group region of a surfactant due to isolation of the polymerisable moiety from the interfacial area. The so formed polymer's phase progression is found to be altered from that of the monomer due to a change in the nature of the paraffinic chains.

As well as this combination affecting the surfactant's self-assembling behaviour at high surfactant compositions the dilute region is also affected due to hydrolysis occurring. These influences act together to shift the cmc of Na-10 to a surfactant concentration which is in excess of the cmcs obtained for surfactants with a quaternary ammonium head group.

Polymerisation of the mesophases formed by Na-10 in water is such that the underlying surfactant geometry is maintained for phases with fluid-like hydrocarbon chains (i.e., the micellar and hexagonal phases) but induces a phase transition (due to disruption of the paraffinic chain order) for phases with frozen hydrocarbon chains.

Therefore, the exact nature of the paraffinic chains (either molten, frozen or bound in a polymer chain) is critical in determining the self-assembly of both the monomeric and polymeric forms of Na-10 and also in the polymerisation of the lyotropic liquid crystalline phases.

Acknowledgments I would like to thank Calum Drummond, Patrick Kékicheff, Stephen Hyde and Maurice Kléman for useful discussions throughout this work. During this work KMM was the recipient of an Australian Postgraduate Research Award.

References

1. McGrath K, Kékicheff P, Kléman M (1993) J Phys II France 3:903–926
2. McGrath K, Drummond C (1995) ibid
3. McGrath K (1995) ibid
4. Small D (1986) The Physical Chemistry of Lipids: From Alkanes to Phospholipids. Handbook of Lipid Research. Plenum Press, New York
5. Sprague E, Duecker D, Larrabee Jr C (1983) J Colloid Interface Sci 92:416–421
6. Levine Y, Wilkins M (1971) Nature New Biology 230:69–76
7. Seelig J (1971) J Am Chem Soc 93: 5017–5022
8. de Gennes P (1974) Phys Lett 47A: 123–124
9. Marcelja S (1974) Biochim Biophys Acta 367:165–176
10. Zaccai G, Blasie J, Schoenborn B (1975) Proc Nat Acad Sci USA 72:376–380
11. Israelachvili J, Marcelja S, Horn R (1980) Quart Rev Biophys 13:121–200
12. Gruen D (1981) J Colloid Interface Sci 84:281–283
13. Gruen D (1985) J Phys Chem 89: 146–153
14. Gruen D (1985) Progr Colloid Polym Sci 70:6–16
15. Ennis J (1992) J Chem Phys 97:663–678
16. Müller A (1930) Proc Roy Soc A127: 417–430
17. Müller A (1932) Proc Roy Soc A138: 514–530
18. Vincent J, Skoulios A (1966) Acta Cryst 20:441–447
19. Vincent J, Skoulios A (1966) Acta Cryst 20:447–451
20. Vincent J, Skoulios A (1966) Acta Cryst 20:432–440
21. Gulik-Kryzwicki T, Rivas E, Luzzati V (1967) J Mol Biol 27:303–322
22. Tardieu A, Luzzati V, Reman F (1973) J Mol Biol 75:711–733
23. Paleos C, Margomenou-Leonidopoulou G, Babilis D, Christias C (1987) Mol Cryst Liq Cryst 146:121–135
24. Durairaj B, Blum F (1989) Langmuir 5:370–372
25. Ekwall P (1927) Acta Acad Aboensis (Math Phys) 4:6
26. Powney J (1935) Trans Faraday Soc 31:1510–1521
27. Powney J, Jordan D (1938) Trans Faraday Soc 34: 363–371
28. Powney J, Addison C (1938) Trans Faraday Soc 34:372–377
29. Powney J, Addison C (1938) Trans Faraday Soc 34:358–363
30. Stainsby G, Alexander A (1949) Trans Faraday Soc 45:585–597
31. Cook M (1951) J Phys Chem 55:383–402
32. Mukerjee P, Mysels K, Dulin C (1958) J Phys Chem 62:1390–1396
33. Eagland D, Franks F (1961) Nature 191:1003–1004
34. Kurz J (1962) J Phys Chem 66: 2239–2246
35. Campbell A, Lakshminarayanan G (1965) Can J Chem 43:1729–1737
36. Lucassen J (1966) J Phys Chem 70:1824–1830
37. Laskowski J (1993) J Colloid Interface Sci 159:349–353
38. Larrabee Jr C, Sprague E (1979) J Polym Sci: Polym Lett Ed 17:749–751
39. Paleos C, Stassinopoulou C, Malliaris A (1983) J Phys Chem 87:251–254
40. Larrabee Jr C, Sprague E (1986) J Colloid Interface Sci 114:256–260
41. Chu D, Thomas J (1991) Macromolecules 24:2212–2216
42. Rosevear F (1954) J Am Oil Chem Soc 31:628–639
43. Rosevear F (1968) J Soc Cosmetic Chemists 19:581–594
44. Kléman M, Colliex C, Veyssié M (1976) In: Friberg S, (ed.) Lyotropic Liquid Crystals and the Structure of Biomembranes. American Chemical Society, Washington, DC, pp 71–84
45. Allain M, Kléman M (1987) J Phys France 48:1799–1807
46. Boltenhagen P, Lavrentovich O, Kléman M (1991) J Phys II France 1: 1233–1252
47. Rosenblatt C, Pindak P, Clark N, Meyer R (1977) J Phys France 38:1105–1115
48. Asher S, Pershan P (1979) J Phys France 40:161–173
49. Rogers J, Winsor P (1969) J Colloid Interface Sci 30:500–510
50. Luzzati V (1968) In: Chapman D, (ed.) Biological Membranes: Physical Fact and Function. Academic press, London, pp 71–123
51. van Voorst Vader F (1961) Trans Faraday Soc 110–115
52. Mysels K, Kapauan P (1961) J Colloid Sci 16:481–483
53. Debye P (1949) J Phys Colloid Chem 53:1–8
54. Campbell A, Bock E (1958) Can J Chem 36:330–338
55. McGrath K (1995) Langmuir 11: 1835–1839
56. Sprague E, Duecker D, Larrabee Jr C (1981) J Am Chem Soc 103:6797–6800
57. Durairaj B, Blum F (1985) J Colloid Interface Sci 106:561–564
58. Gambogi R, Blum F (1990) J Colloid Interface Sci 140:525–534
59. Shibasaki Y, Fukuda K (1992) Colloids and Surfaces 67:195–201
60. Denton J, Duecker D, Sprague E (1993) J Phys Chem 97:756–762
61. Friberg S, Thundathil R, Stoffer J (1979) Science 205:607–608
62. Thundathil R, Stoffer J, Friberg S (1980) J Polym Sci: Part A: Polym Chem Ed 18:2629–2640